

Supporting Information

Spontaneous Resolution of Two Homochiral Ferroelectric Cadmium(II) Frameworks and an Achiral Framework from an One-pot Reaction Involving Achiral Rigid Ligands

Zhi Su, Man-Sheng Chen, Jian Fan, Min Chen, Shui-Sheng Chen, Li Luo, Wei-Yin Sun*

Coordination Chemistry Institute, State Key Laboratory of Coordination Chemistry, School of Chemistry and Chemical Engineering, Nanjing National Laboratory of Microstructures, Nanjing University, Nanjing 210093, China. E-mail: sunwy@nju.edu.cn; Fax: +86 25 8331 4502

Table S1. Selected Bond Lengths (Å) and Bond Angles (°) for Complex **1 - 2**

Complex 1L^a			
Cd1-N1	2.272(5)	Cd1-N5#2	2.440(5)
Cd1-N3#1	2.278(4)	Cd1-O1	2.308(4)
Cd1-O2	2.612(5)	Cd1-O3#3	2.504(5)
Cd1-O4#3	2.447(5)		
O1-Cd1-O2	52.19(14)	O2-Cd1-N3#1	82.34(15)
O1-Cd1-N1	97.00(17)	O2-Cd1-O3#3	159.05(16)
O1-Cd1-N5#2	79.23(17)	O2-Cd1-O4#3	141.95(16)
O1-Cd1-N3#1	133.89(16)	N1-Cd1-N5#2	167.92(17)
O1-Cd1-O3#3	136.38(16)	N1-Cd1-N3#1	95.60(17)
O1-Cd1-O4#3	89.76(16)	O3#3-Cd1-N1	100.07(17)
O2-Cd1-N1	96.92(16)	O4#3-Cd1-N1	86.61(16)
O2-Cd1-N5#2	89.83(16)	N3#1-Cd1-N5#2	95.22(17)
O3#3-Cd1-N3#1	83.89(16)	O3#3-Cd1-N5#2	75.78(17)
O4#3-Cd1-N3#1	135.21(16)	O4#3-Cd1-N5#2	81.93(16)
O3#3-Cd1-O4#3	51.92(16)		

Complex 1R^b

Cd1-N1	2.275(3)	Cd1-N5#2	2.444(4)
Cd1-N3#1	2.280(4)	Cd1-O1	2.311(3)
Cd1-O2	2.621(4)	Cd1-O3#3	2.507(4)
Cd1-O4#3	2.434(3)		
O1-Cd1-O2	52.39(11)	O2-Cd1-N3#1	82.13(12)
O1-Cd1-N1	96.68(12)	O2-Cd1-O3#3	158.93(12)
O1-Cd1-N5#2	79.62(12)	O2-Cd1-O4#3	142.06(12)
O1-Cd1-N3#1	133.86(12)	N1-Cd1-N5#2	168.31(12)
O1-Cd1-O3#3	136.69(12)	N1-Cd1-N3#1	95.66(13)
O1-Cd1-O4#3	89.67(12)	O3#3-Cd1-N1	100.32(12)
O2-Cd1-N1	96.48(12)	O4#3-Cd1-N1	86.83(12)
O2-Cd1-N5#2	90.03(12)	N3#1-Cd1-N5#2	94.84(13)
O3#3-Cd1-N3#1	83.64(12)	O3#3-Cd1-N5#2	75.75(13)
O4#3-Cd1-N3#1	135.32(13)	O4#3-Cd1-N5#2	82.09(12)
O3#3-Cd1-O4#3	52.25(12)		

Complex 2^c

Cd1-O1W	2.237(3)	Cd2-N3	2.262(4)
Cd1-O7#3	2.256(4)	Cd2-N1#1	2.263(3)
Cd1-N5#2	2.295(4)	Cd2-O1	2.318(3)
Cd1-O3	2.310(4)	Cd2-O6	2.380(3)
Cd1-O4	2.355(3)	Cd2-O2	2.384(3)
Cd1-O8#3	2.535(3)	Cd2-O5	2.404(3)
O1W-Cd1-O7#3	124.21(14)	N3-Cd2-N1#1	101.81(13)
O1W-Cd1-N5#2	102.01(13)	N3-Cd2-O1	98.18(12)
O7#3-Cd1-N5#2	89.32(14)	N1#1-Cd2-O1	127.33(13)
O1W-Cd1-O3	121.36(14)	N3-Cd2-O6	109.56(12)
O7#3-Cd1-O3	114.12(16)	N1#1-Cd2-O6	86.85(12)
N5#2-Cd1-O3	83.22(13)	O1-Cd2-O6	130.33(11)
O1W-Cd1-O4	92.34(13)	N3-Cd2-O2	150.91(12)
O7#3-Cd1-O4	115.26(15)	N1#1-Cd2-O2	87.50(12)
N5#2-Cd1-O4	137.33(13)	O1-Cd2-O2	55.78(11)
O3-Cd1-O4	55.46(12)	O6-Cd2-O2	98.32(11)
O1W-Cd1-O8#3	84.83(12)	N3-Cd2-O5	92.15(12)
O7#3-Cd1-O8#3	53.92(12)	N1#1-Cd2-O5	141.56(12)
N5#2-Cd1-O8#3	136.52(13)	O1-Cd2-O5	84.79(11)
O3-Cd1-O8#3	129.73(13)	O6-Cd2-O5	54.71(10)
O4-Cd1-O8#3	84.16(12)	O2-Cd2-O5	97.45(11)

^aSymmetry transformations used to generate equivalent atoms: #1 1-y, 1+x, -1/4+z; #2 1+x, 1+y, z; #3 y, 3-x, 1/4+z.

^bSymmetry transformations used to generate equivalent atoms: #1 3+y, 1-x, -1/4+z; #2 1+x, 1+y, z; #3 2-y, -2+x, 1/4+z.

^cSymmetry transformations used to generate equivalent atoms: #1 x, -1+y, z; #2 1+x, -1+y, 1+z; #3 2+x, -1+y, z.

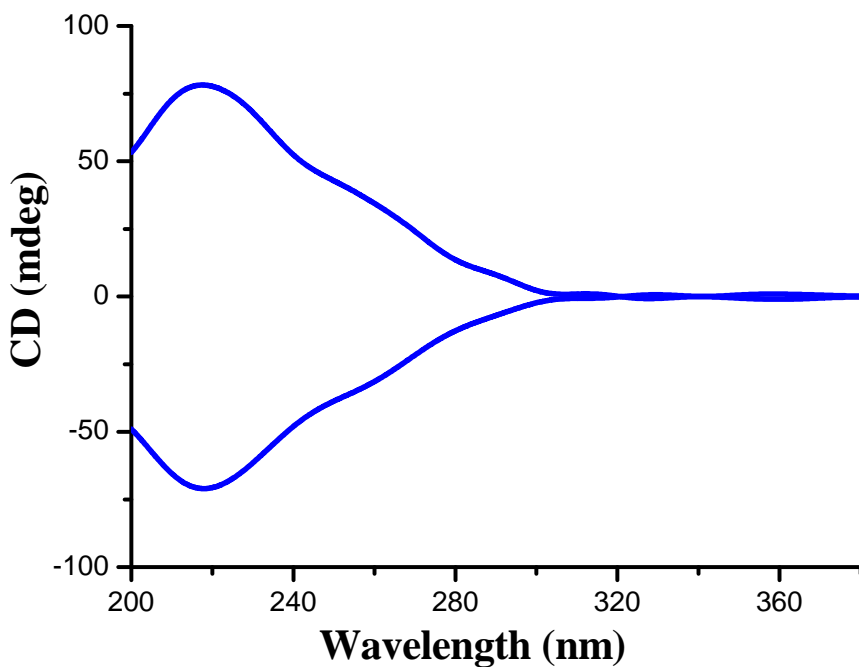


Figure S1. Solid-state CD spectra of complex **1** (KBr pellet).

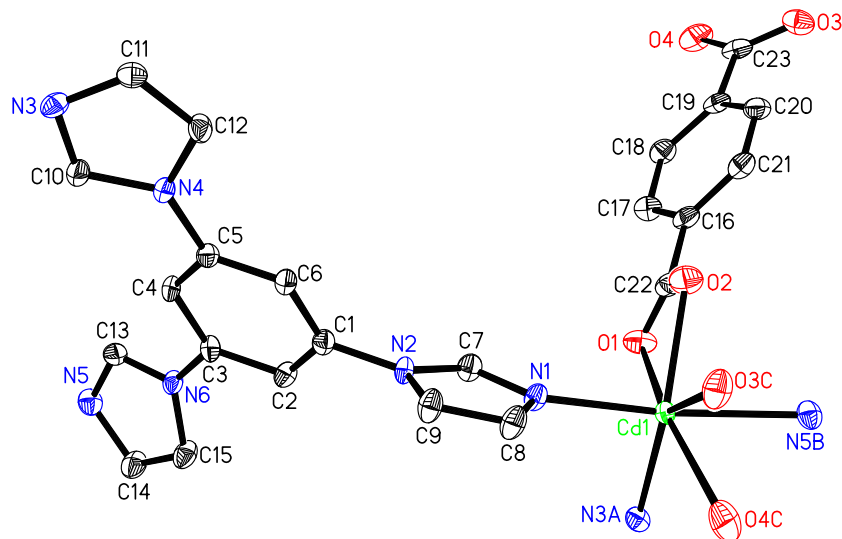


Figure S2. The asymmetric unit of complex **1L** with the ellipsoids drawn at the 30 % probability level. The hydrogen atoms and free water molecules are omitted for clarity.
Symmetry code: A, 1-y, 1+x, -1/4+z; B, 1+x, 1+y, z; C, y, 3-x, 1/4+z.

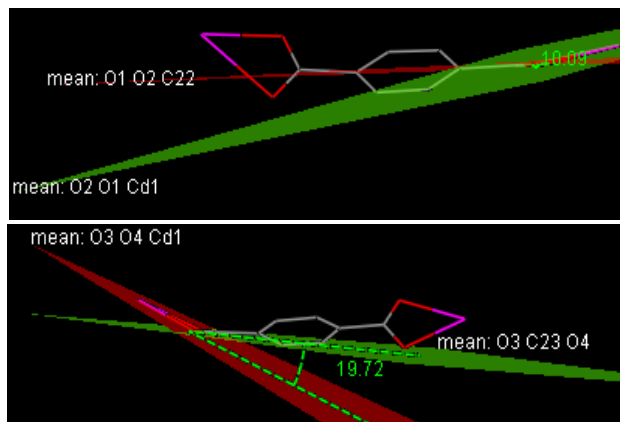


Figure S3. The distortion of BDC^{2-} in **1**.

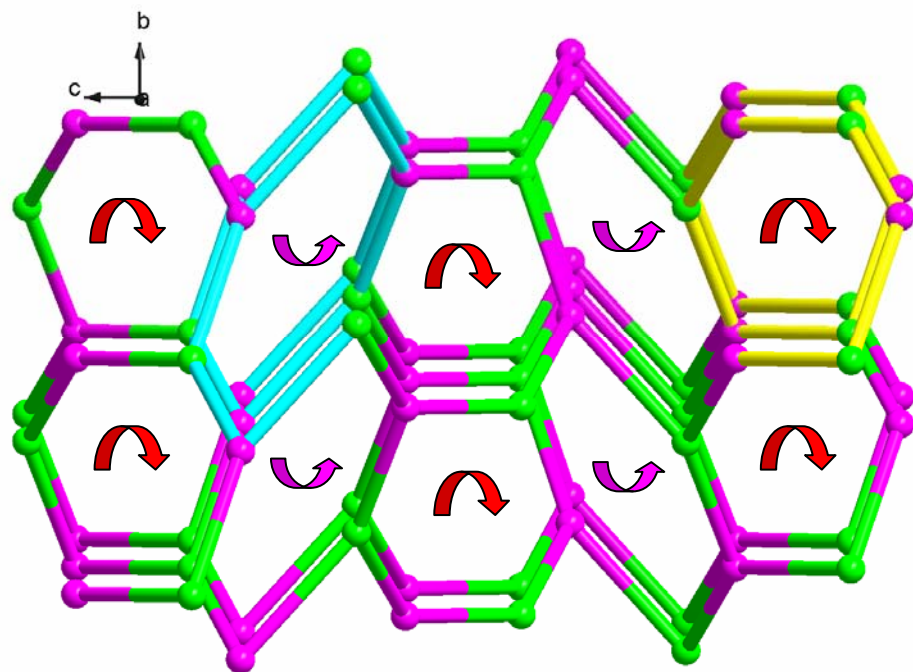


Figure S4. Schematic representation of the (10, 3)-b along the a axis (Pink balls: tib ligands; Green balls: Cd(II) atoms).

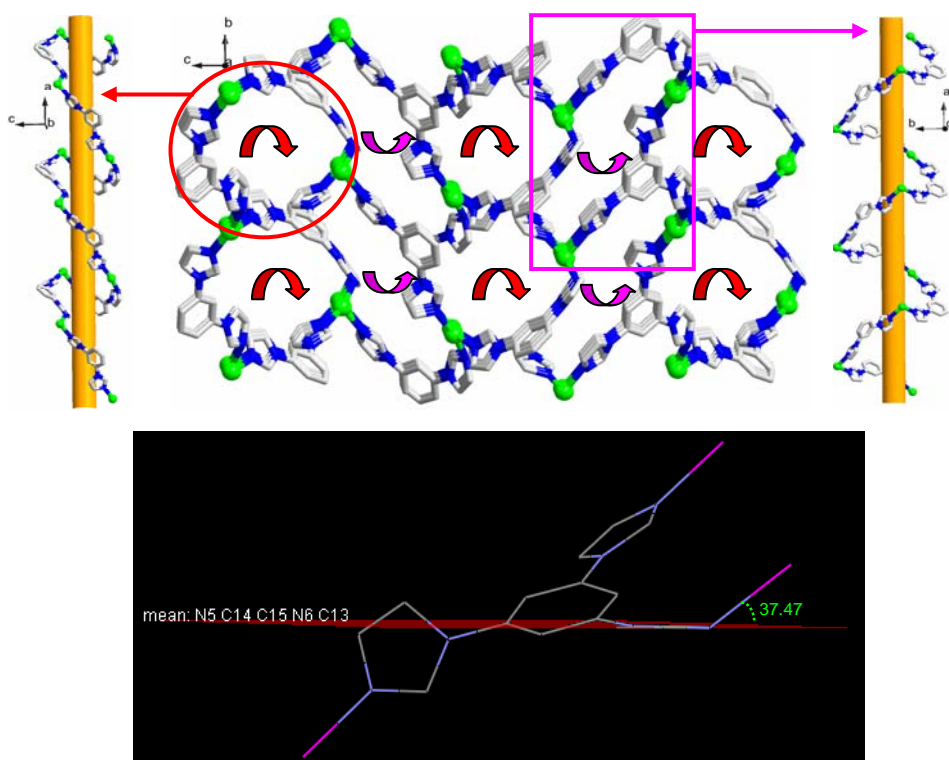


Figure S5. View of the 3D (10, 3)-b net constructed by tib and Cd(II) along *a* axis, in which the narrow are represent the direction of the helical chains (top). The distortion of tib is highlighted (bottom).

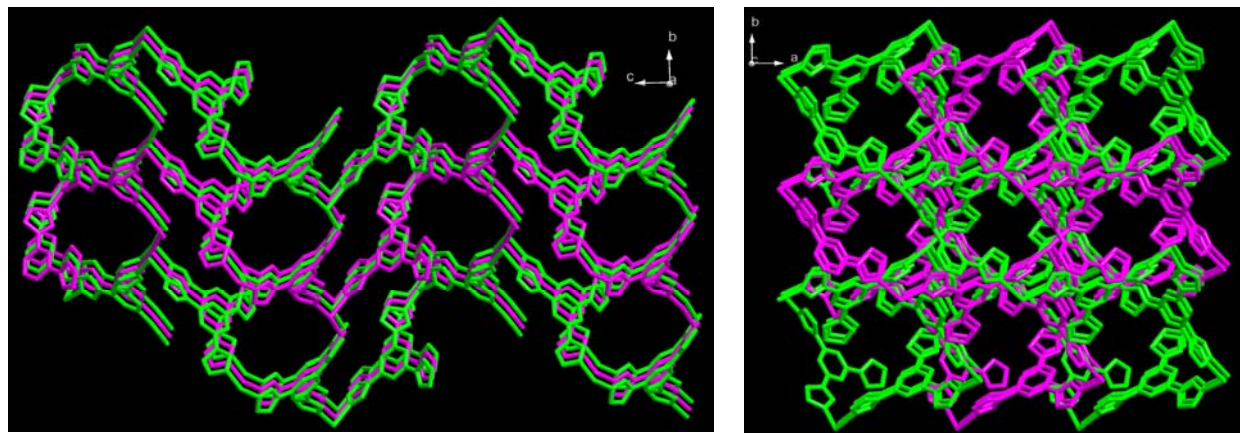


Figure S6. The 2-fold interpenetrating 3D structure of tib-Cd(II) viewed along *a* axis (left) and *c* axis (right), respectively.

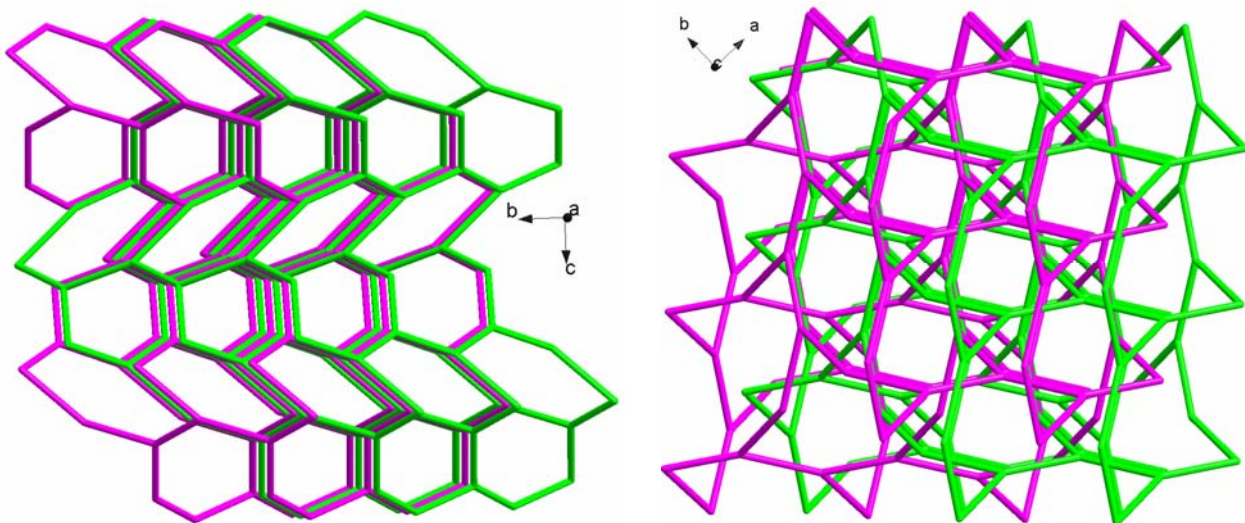


Figure S7. The 2-fold interpenetrating (10, 3)-b net viewed along *a* axis (left) and *c* axis (right), respectively.

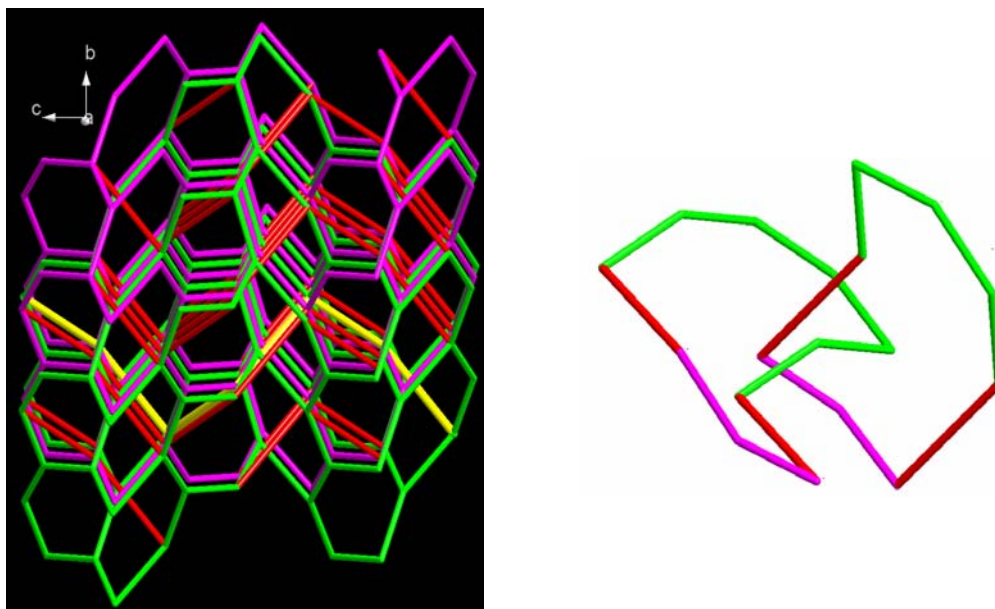


Figure S8. Left: the topological representation of the ultimate structure of **1L**, in which the pink and green lines are represented the 2-fold interpenetrating (10, 3)-b nets and the red and high-highlighted yellow lines are for the left-handed helical chains. Right: the close-up view of self-penetrated rings in **1L**.

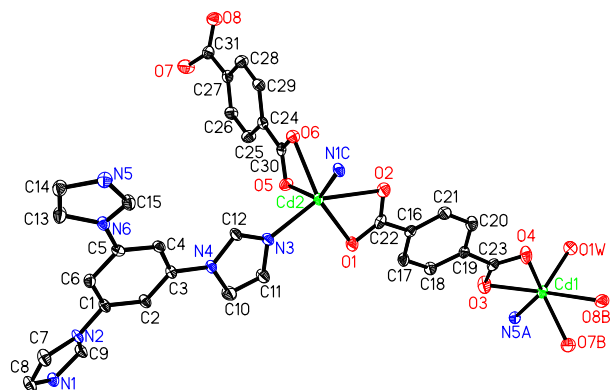


Figure S9. The asymmetric unit of complex **2** with the ellipsoids drawn at the 30 % probability level. The hydrogen atoms and free water molecules are omitted for clarity.
Symmetry code: A, $1+x, -1+y, 1+z$; B, $2+x, -1+y, z$; C $x, -1+y, z$.

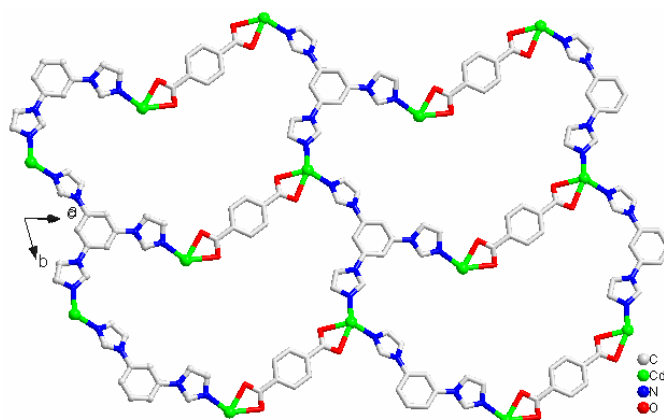


Figure S10. The 48-membered ring in the 2D layer constructed by tib, BDC and Cd(II) atoms in **2**.

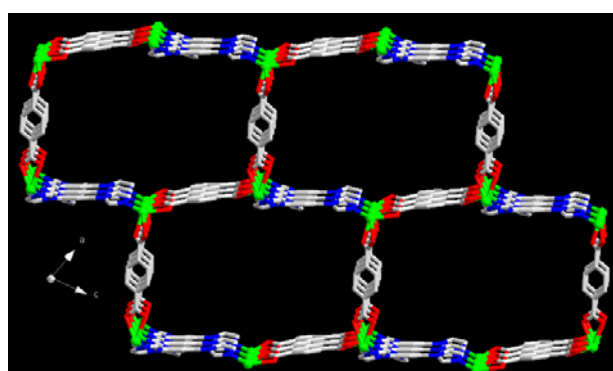


Figure S11. The 3D structure of **2** with 1D open channels.

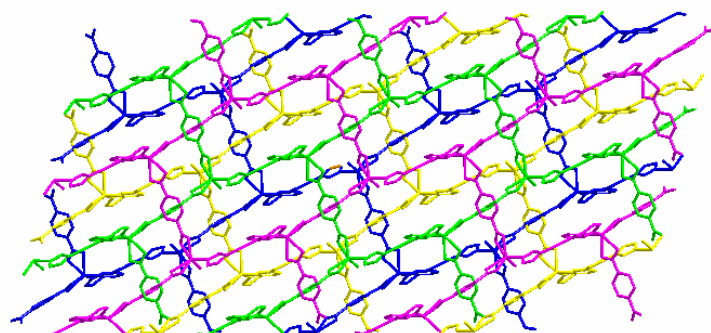


Figure S12. The 4-fold interpenetrating structure of **2**.

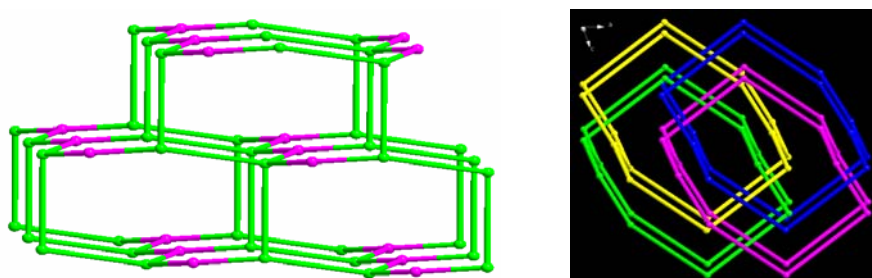


Figure S13. Left: the representation of the **tfa** topology of **2**, in which the pink balls are for the tib ligands and the green balls for the Cd(II) atoms. Right: the 4-fold interpenetrating **tfa** net of **2**.

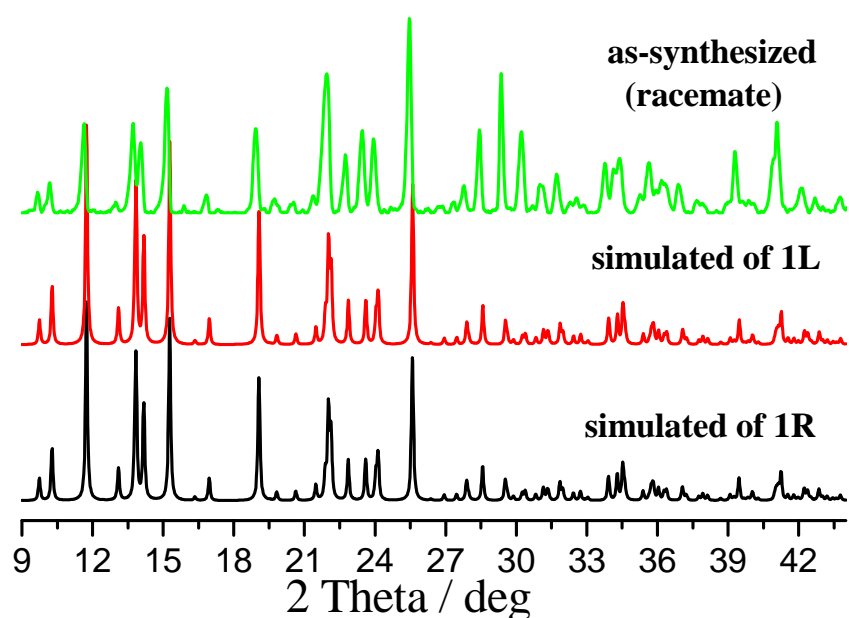


Figure S14. The as-synthesized and simulated XRD data of complex **1**.

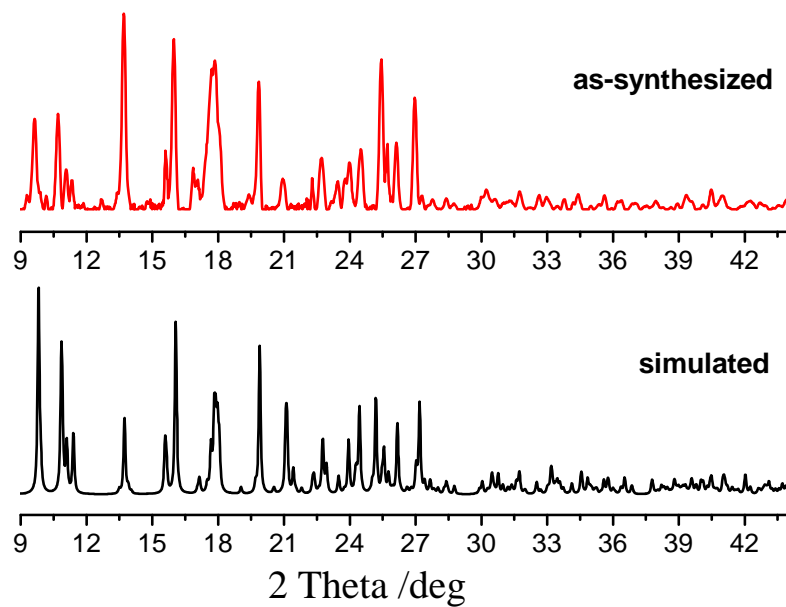


Figure S15. The as-synthesized and simulated XRD data of complex **2**.

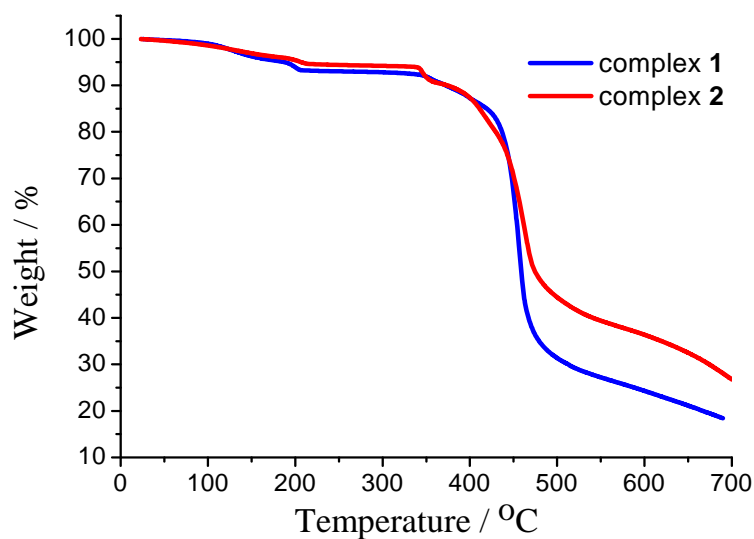


Figure S16. The TG curves of **1** and **2**.